Emergent bursting and synchrony in computer simulations of neuronal cultures

Niru Maheswaranathan[1], Silvia Ferrari[2], Antonius M.J. VanDongen[3] and Craig S. Henriquez[1*]

Abstract

Experimental studies of neuronal cultures *in vitro* have revealed a wide variety of spiking network activity ranging from sparse, asynchronous firing to distinct, network-wide synchronous bursting. However, the functional mechanisms driving these observed firing patterns is not well understood. In this work, we have developed an *in silico* network of cortical neurons based on known features of similar *in vitro* networks. The activity from these simulations is found to closely mimic experimental data. Furthermore, the strength or degree of network bursting is found to depend on a few parameters: the density of the culture, the type of synaptic connections, and the ratio of excitatory to inhibitory connections. Network bursting gradually becomes more prominent as either the density, the fraction of long range connections, or the fraction of excitatory neurons is increased. Interestingly, typical values of parameters result in networks that are at the transition between strong bursting and sparse firing. Using a measure of network entropy, we show that networks with typical parameters have maximum information capacity due to the balance between redundancy to reduce noise and variability for efficient coding. These results have implications for understanding how information is encoded at the population level as well as for why certain network structures are ubiquitous in cortical tissue.

Keywords Neuronal cultures, Bursting, Computer simulations, Synchrony, Network Entropy, Small-world networks

[1]Dept. of Biomedical Engineering, Duke University, Durham, NC, USA
[2]Dept. of Mechanical Engineering and Materials Science, Duke University, Durham, NC, USA
[3]Program in Neuroscience & Behavioral Disorders, Duke-NUS Graduate Medical School
[*]Correspondance: Craig Henriquez, 136 Hudson Eng Ctr, , Durham, NC, 27708, USA. E-mail: ch@duke.edu

1 Introduction

With the development of multielectrode arrays (MEAs), researchers are able to record extracellularly from large sets of cultured neurons *in vitro.* Typical MEAs consist of a matrix of very tiny electrodes (around $30\mu m$ in diameter, spaced around $200\mu m$ apart) embedded in a two-dimensional grid. Cortical tissue from animal models, typically rodents, is plated onto the arrays and allowed to grow and differentiate on the electrodes, and can last for weeks or months at a time [9]. Neurons quickly form synaptic connections with one another and develop into fully functioning networks. The electrical activity of these networks is then recorded extracellularly using the embedded electrodes. These techniques allow for relatively high spatial and precise temporal resolution while recording from of a culture, yielding access to the spiking activity of a subset of neurons in the culture. MEAs have been used to observe and characterize the wide variety of bursting activity that is present in cortical cultures [12].

Bursting is the most prevalent behavior observed in these culture. Activity ranges from sporadic, asynchronous firing to periodic, synchronous network bursts. This network bursting is found to be robust and is observed in multiple experimental setups [3]. Despite vast experimental data, the mechanisms that govern network bursting *in vitro* are unclear, in part because all parameters of interest cannot be precisely controlled. There is experimental evidence to suggest that the plating density of a culture as well as the culture's age play an significant role in determining the amount of synchronization in the network [12]. There is a growing body of knowledge regarding the structure of such networks. For example, biological neural systems have been shown to obey the small-world connection paradigm proposed by Watts and Strogatz [13]. A recent study by Gerhard et. al. [5] showed that the topology of cortical cultures shows a small but significant small-world structure, and that distance-dependent connectivity can account for the small-world effect. Other studies have also observed the presence of small-world structure in neural networks [11, 1].

In order to further understand the biophysical mechanisms behind observed behavior of *in vitro* networks, an *in silico* model of a typical neuronal culture was developed, allowing parameters of interest to be varied systematically. The model simulates a 2D medium of spiking neurons with variable axonal delays, exponentially decaying synapses, and small world connections. In addition, the electrode interface of the MEA is modeled for direct comparison with experimental data. A wide variety of activity patterns emerge in the simulations which closely mimic activity seen *in vitro.* The strength of emergent network bursting, characterized

by burst rate and periodicity, is explored across the parameter space. In addition, information theoretic analysis is applied to quantify the ability of a network to maximally encode a signal in the presence of noise and provide some insight into the nature of neural coding through the use of bursts. Results show that bursting is an emergent phenomenon as density, long-rage connections, and the fraction of excitatory neurons are increased, and that the critical region for when bursting develops occurs at parameter values typically observed in cultures. Furthermore, a measure of the information contained in the network shows that information capacity peaks at the onset of network bursting, thus providing a reason for why such parameter values are observed.

2 Materials and Methods

2.1 Spiking neuron model

The framework of the model consists of a set of N interconnected spiking neurons. To accurately capture the varied behavior present in neuronal populations while maintaining computational efficiency, the Izhikevich model was used to simulate the spiking dynamics of each neuron [6]. The Izhikevich model consists of a fast acting variable describing the membrane voltage (v) and a slowly decaying membrane reset variable (u), and four dimensionless parameters (a, b, c and d) allow for tuning of the spiking behavior of the neurons. BRIEFLY EXPLAIN WHAT YOU FOUND WITH INTEGRATE AND FIRE NEURONS AND WHY THEY WERE NOT USED HERE.

Each neuron in the network is assigned values for the parameters a through d depending on whether the neuron is excitatory or inhibitory. Excitatory neurons are modeled as typical regular spiking neurons, and inhibitory are modeled as fast spiking neurons. In addition, a stochastic component to these parameters was included to encourage varied spiking dynamics throughout the network. For a detailed description of the model and the data analysis methods described below, see the appendix.

2.2 Network connections

Connections between neurons are formed via synapses modeled with a single variable, n, representing the amount of neurotransmitter release at the synapse. The amount of neurotransmitter decays exponentially, and is released instantaneously as an action potential reaches the presynaptic terminal. Axonal delays are ran-

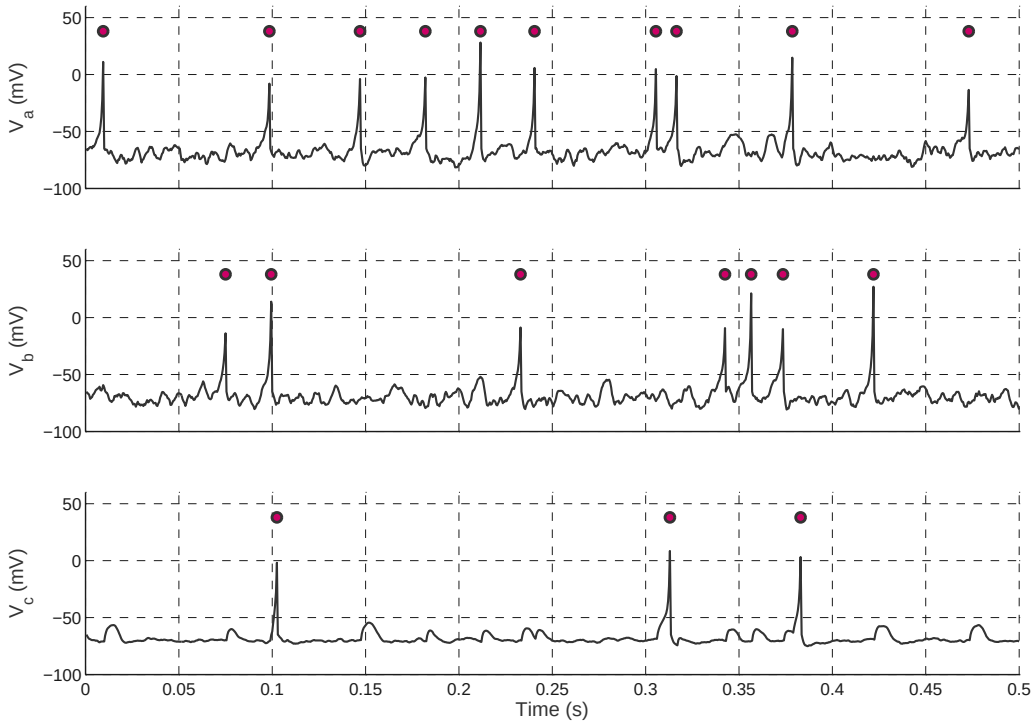

Figure 1: Interactions between three neurons. Neuron a (top trace) and b (middle trace) are presynaptic neurons that terminate onto c (bottom trace). Voltage traces (lines) and spikes (circles) for neurons a, b and c during 0.5s of simulation are shown. Note that coincidental spikes from a and b are will cause c to fire, and only occasionally will a spike from one presynaptic neuron but not the other causes c to fire.

domly chosen from a normal distribution and assigned to each neuron. In the model, neurons are treated as points embedded in a two-dimensional medium, which serves as the surface of the multielectrode array. Figure 1 shows voltage traces of three simulated Izhikevich neurons at a synapse, with two excitatory neurons synapsing onto the third.

Neurons are connected according to the small-world paradigm proposed by Watts and Strogatz [13]. Neurons are initially connected to every neuron within some radius threshold, and then randomly reconnected to other neurons across the network with probability p. Note that for small values of p, the network is ordered but highly localalized (characterized by a large clustering coefficient and a large mean path length), while for large values of p the network is largely randomized

Parameter	Description	Value
d_n	Neuron density	$250 \frac{neurons}{mm^2}$
p	Small-world rewiring probability	0.03
$N_e : N_i$	Ratio of excitatory/inhibitory connections	4:1
σ^2_{noise}	Noise variance	1.5
e_{rad}	MEA electrode radius	$25\mu m$
e_{sep}	MEA electrode separation distance	$200\mu m$
dt	Simulation time step	$0.5ms$
$d_{min} - d_{max}$	Axonal conduction delay range	$2ms - 20ms$
τ_{syn}	Synaptic time constant	$2ms$

Table 1: Neural network and simulation parameters

(characterized by a small clustering coefficient and short mean path length). A network is considered "small-world" if it fits between these two regimes, thus if it has a short mean path length and large clustering coefficient. Figure 2 shows the effect of this probability on the network. A value of $p = 0.03$ was chosen to obtain a short mean path length and high clustering coefficient. This process yields sparse synaptic weight distributions which are then initialized to randomly chosen weights, drawn from normal distributions. The model incorporates both excitatory and inhibitory synapses, with fractions that can be varied.

2.3 Simulations and MEAs

Each single trial consists of generating a newly randomized network with a unique set of weights, connections, and neuronal parameters. The network is then simulated using random synaptic noise as the only input. In addition to recording the spike times of all of the individual neurons, the electrode interface of the multi-electrode arrays is modeled as well. MEAs are modeled with a 7×8 grid of electrodes spaced $200\mu m$ apart. Each electrode records spikes from neurons within a $20\mu m$ radius of the center of the electrode, and in total they capture a small subset of the spiking activity of the whole network. For simplicity, it is assumed that the spike time can be detected at the electrode, but sorting of the contributing neurons is not performed (NOT SURE IF THIS IS CORRECT).

The model was developed in Matlab (The MathWorks Inc., Natick, MA) using C++ `mex` files as the core. This allows for simulation of around 800 neurons in real time on a 2GHz computer. Table 1 shows a list of parameters used and their values.

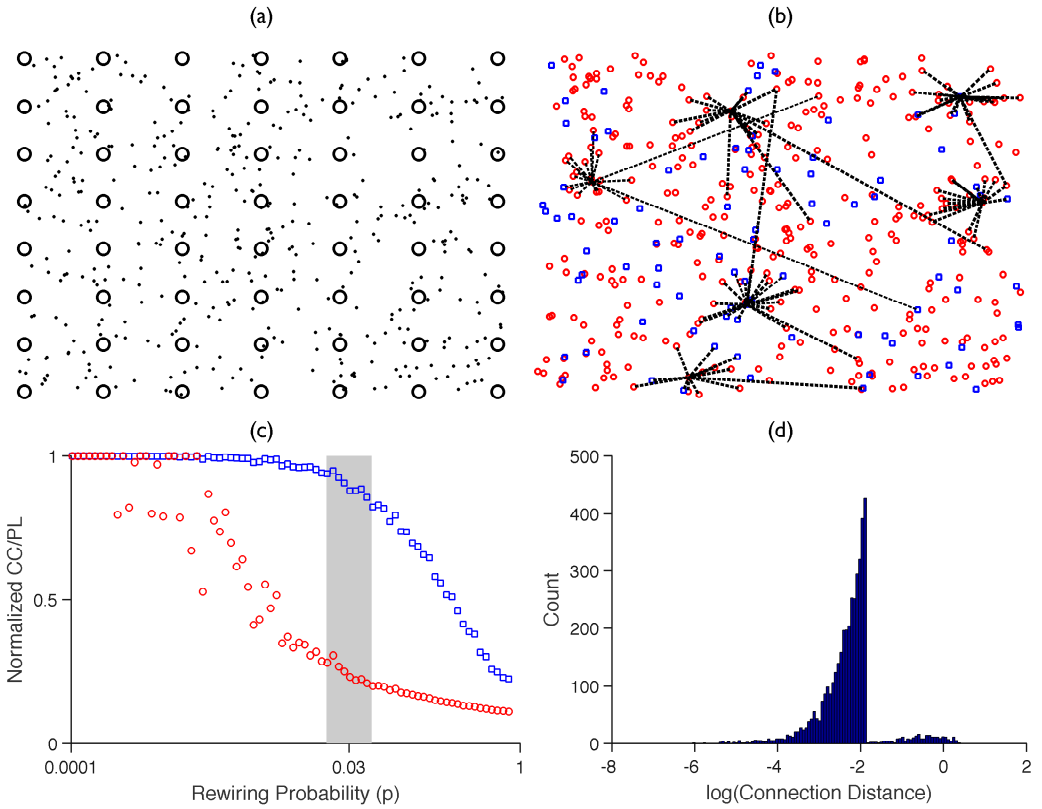

Figure 2: Small-world network connections. (a) Neurons (dots) are placed in random locations of a 2D medium, along with the embedded electrodes (circles). (b) Excitatory (circles) and inhibitory (squares) neurons shown with connections (dashed lines) drawn for seven randomly chosen neurons. Note that some connections are long range but the majority lie within a given radius threshold. (c) Characteristic path length (circles) and clustering coefficient (squares) in networks as a function of the probability of rewiring, p. A p value of 0.03 was chosen for a large clustering coefficient and small path length, characteristic of small-world networks. (d) Histogram of the log of the distance of synaptic connections. Most connections are short ($10^{-2}mm$ or less) though some are long range (around $1mm$).

2.4 Data analysis

In order to measure the degree or amount of network synchronization or bursting present in a given simulation, two different metrics were used: the maximum AC component (MAC) and the bursts per minute count (BPM). In order to compute these estimates across N different spike trains for a network with N neurons, all of the spikes are binned using discrete time windows to obtain a time-varying signal corresponding to the average firing rate of the entire network at a given point in time. This signal is then normalized by the mean firing rate and smoothed by convolving with a Gaussian kernel. The filtered signal is defined as the global firing rate, or GFR. The GFR is a time varying signal that represents the firing rate of the network over time.

For networks that display prominent synchronized bursting, this signal has sharp peaks during the bursts as many neurons in the network are firing in a short time window. To quantify the rate of bursting independent of whether it is synchronous or not, the GFR signal is used. A peak detection algorithm is run on the GFR and the number of peaks found per minute is computed and defined as the bursts per minute (BPM) count. The more prominent a network burst is, the sharper the peak will be in the GFR signal, and the more likely it is to be registered in the BPM count. To compute the MAC parameter, frequency analysis is used. The Fourier spectrum of the GFR signal is analyzed by computing the fast Fourier transform (FFT). The FFT is then normalized by setting the DC (zero frequency) component of the FFT to 1. The amplitude of the maximum AC (nonzero frequency) component of this signal is defined as the maximum AC (MAC) parameter. A high value for the MAC parameter corresponds to a high degree of synchrony in the network, as there is a sharp peak in the normalized FFT. The frequency at which the maximum value occurs indicates the fundamental frequency of network bursting. The MAC serves as a measure of the periodicity of network bursting. Figure 3 shows these metrics applied to example sets of spike trains.

2.4.1 PCA and Information theory

Previous work [4] has used dimensional reduction techniques to project firing rates onto low-dimensional variables that allow for easier visualization of neural trajectories. The general idea is that redundancy is encoded in the firing rates of neurons, so using a PCA-like method to transform the firing rates onto a basis that better captures the variance in the data allows us to ignore the redundant variables. To extract neural trajectories, the firing rates for individual neurons were first

determined by binning spike counts into 10*ms* time windows. The square root of the rates was taken (to compress the range) and then smoothed by convolving the signals with a Gaussian kernel. PCA was run on these smoothed firing rate trajectories, and the top three components were extracted to serve as the low-dimensional projection of the neural state.

The PCA method described above assumes that the information in the network

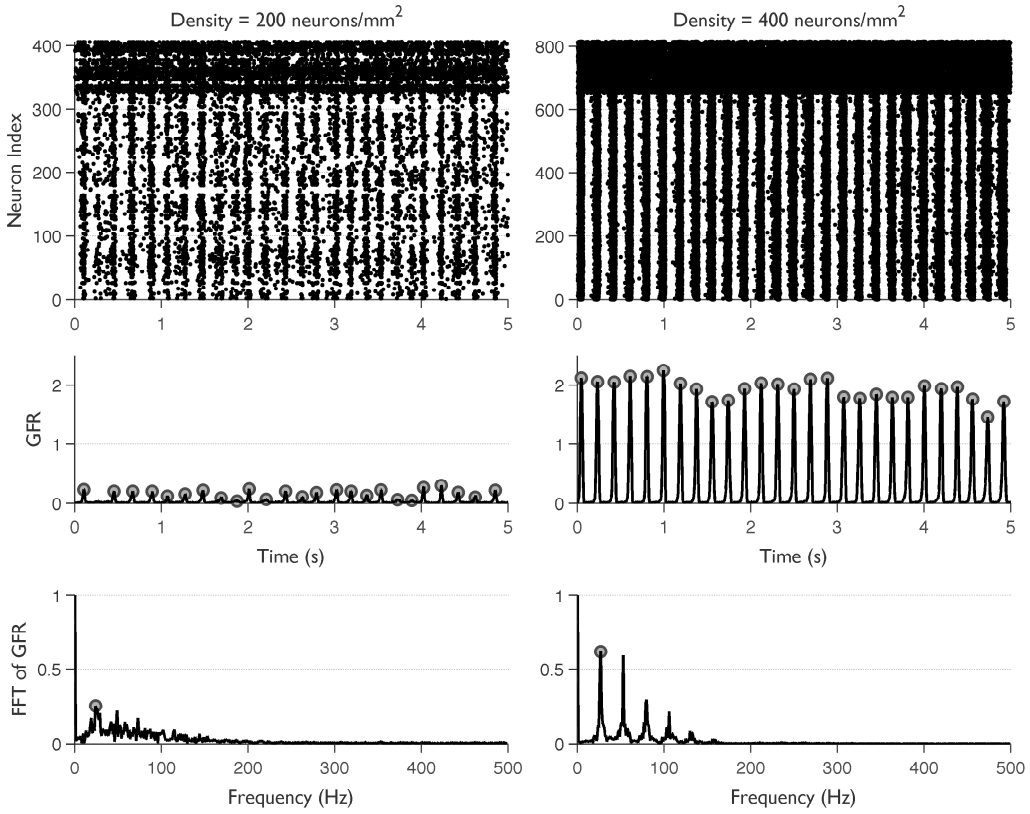

Figure 3: Example of metrics used to characterize degree of bursting. Metrics shown for a low density network (left, 200 neurons/mm^2) and a high density network (right, 400 neurons/mm^2). Top: Rasters of the spiking activity of all neurons in the network for 5s of simulation. Inhibitory neurons are located at the top, and fire more rapidly. Middle: Global firing rate (GFR) signal along with bursts detected through peak detection using the GFR signal. Bottom: Fourier transform of the GFR shown, normalized by the DC component. The higher density network has a larger maximum AC component of the GFR.

is described by the instantaneous firing rate. In order to more rigorously quantify the amount of information carried within a given network, we turn to information theory. Yu et. al. [14] proposed a Fourier-based method of computing the information delivery rate from a population of neurons which we use here to estimate the information carrying capacity of a given network. It consists of treating each spike train as a series of delta functions, where each is shifted in time to the location of a given spike. The fourier transform of a set of such delta functions is a sum of sines and cosines whose frequency depend on the timing of the spike. These fourier coefficients allow for estimation of the entropy at each frequency in the network. With enough data, the set of fourier coefficients at a given frequency approaches a normal distribution according to the central limit theorem. The entropy of a normal distribution is then computed given the variance of that distribution. The total entropy of the network is given by summing across all frequencies.

If we have a network of multiple neurons, then the distribution of fourier coefficients is a multivariate gaussian and is characterized by its covariance matrix. From the covariance, the entropy across frequency and sum across frequency is estimated. For an input that is random noise, this approach gives an estimate of the total entropy of a system [14]. For a repeated input, however, the computation described above yields just the noise entropy. To estimate the information of the network, a simulation was run with random noise and another was run with a repeated stimulus. The difference in entropy between the two was used as the measure of the information of the network.

3 Results

3.1 Qualitative Behavior

Figure 4 shows examples of activity from the simulations: the behavior of all neurons (left) and those that are recorded at the simulated electrodes (right). Note the large variability in activity (here shown across different network densities), indicating that the transition from spare asynchronous activity to network bursting is gradual. Spatial subsampling of MEA electrodes seems to capture the qualitative behavior but fails to capture a large amount of the activity in the network. Activity patterns are robust with respect to the random initialization of the network, that is, the observed bursting occurs independently of the initial connections, weights, and neuronal properties of the network.

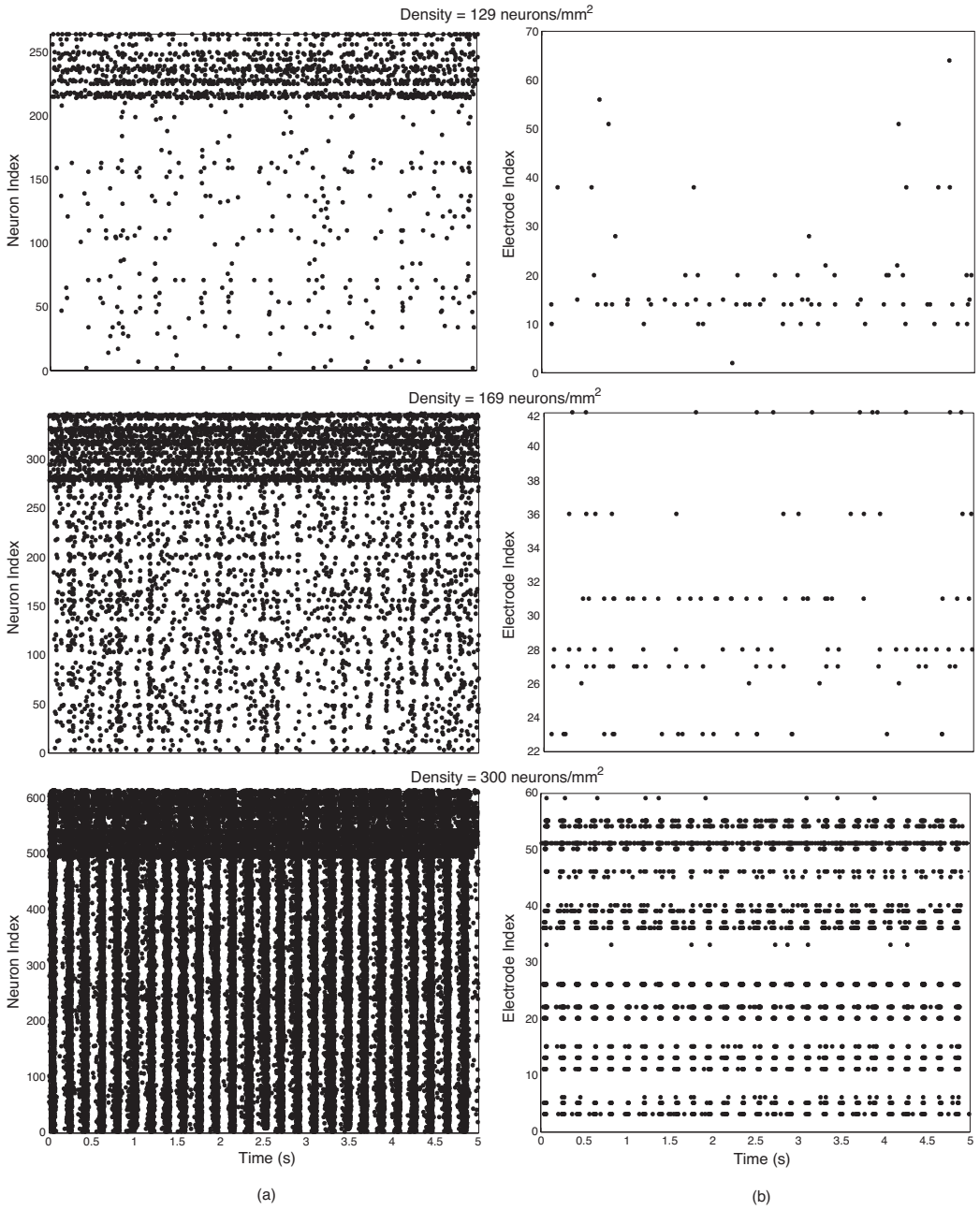

Figure 4: Network activity and electrode recordings from simulation. Rasters of both the spiking activity of all neurons (a) and that recorded by the simulated MEA (b) across 5*s* of simulation. Three different networks are shown, one of a low density (top), medium density (middle), and high density (low). The high firing rates for the upper neuron indices correspond to the fast spiking inhibitory neurons, which have different dynamics than the excitatory neurons. Network bursting gradually becomes more pronounced as density is increased.

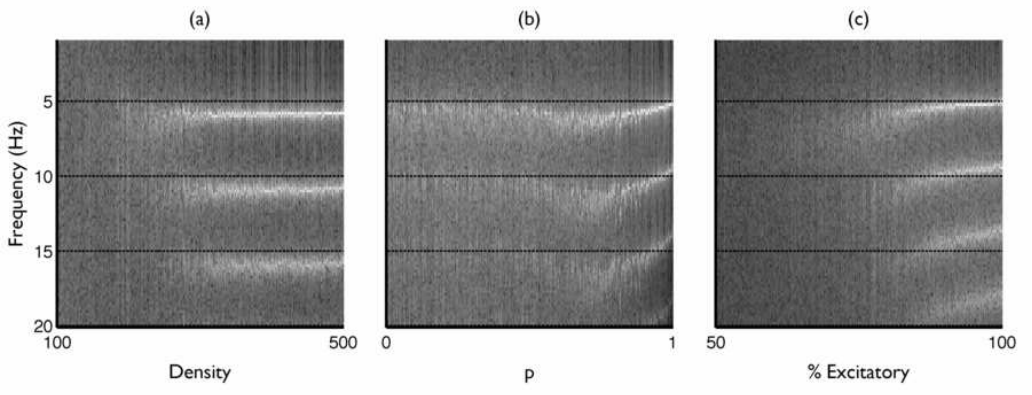

Figure 5: FFT of GFR signal across different parameters. Images show emergence of synchronous activity as the (a) density, (b)small-world rewiring probability p, and (c) % of excitatory connections are varied. Largest frequency component emerges for all three parameters around just over 5Hz, corresponding to the frequency of network bursting. The higher values observed in the FFT are harmonics of this 5Hz bursting.

3.2 Variation across parameter space

The effect of three different parameters (density, connection type, and ratio of excitatory/inhibitory connections) on network activity was studied. For each parameter, a range of different values was tested (densities from 100-600 neurons/mm^2, p values from 0.001 to 1, and the fraction of excitatory neurons from 0.5 to 1). Each parameter affects the network structure differently: increasing the density corresponds to an increase in the number of connections each neuron makes, as there are more neurons within the local threshold to form synapses with. Increasing the value of p only affects how the connections are organized: either local and structured (small p) or long-range and disorganized (large p). Finally, increasing the fraction of excitatory neurons affects the amounts of inhibitory and excitatory neurotransmitter release in the network. Each range was tested by generating a new randomized network for each parameter value and simulating with random noise for 5 seconds.

Figure 5 shows the fourier transform of the global firing rate (GFR) signal across parameters. Note that as each parameter is increased, highly periodic structure emerges centered around a fundamental frequency of just over 5Hz. This frequency corresponds to the bursting rate of around five times per second, which

is consistent with observed bursting frequency in cultures. The maximum AC component (MAC) and number of bursts were also computed across the range of parameters. These results are summarized in Figure 6. The vertical grey bar indicates the typical range of the parameter of interest (Table 1). The general trend appears to be that as the network gets denser (more connected) and as those connections are more likely to reach out across the network, there is an increase in synchronous network activity. Perhaps surprisingly, typical networks (grey bar) with respect to all three parameters tend to be centered at the middle of the transition between sparse firing and synchronous bursting.

3.3 Principal components analysis

Principal components of firing rates were computed to better visualize the neural state. Example neural trajectories are shown in Figure 7 for different values of density and of p. Note that as the degree of synchrony in the network increases (for increasing values of p and density) the trajectory projected onto the first principal component becomes increasingly periodic. It is much easier to characterize the synchrony in the system by looking at the projection of the first principal component rather than of the global activity. The motivation behind applying dimensionality reduction technqiues to neural data is to eliminate the redundancy inherent to the neural code and to extract out interesting variables.

Plots of the projection of neural state onto the top three principal components are shown in Figure 8. Here, each point in the space can be thought of as a distinct neural state. The trajectory through the space across time represents the evolution of that neural state. For asynchronous networks (top), the trajectories appear random or chaotic. The neural state is unpredictable using just a three dimensional projection of the original data space. However, for networks that have syncrhonous network bursting (bottom), the trajectories appear to follow some sort of limit cycle or other attractor as they evolve through the space. The evolution of the attractor is again gradual across different values of density or p, but once it develops it remains the same across newly initialized networks with similar properties.

These results also make sense when we look at how much variance is captured by the first principal component across the parameter space, shown in Figure 9. For large values of p or high densities, there is a large amount of redundancy in the system, and the neural state can be approximated with just a few variables. This seems rather inefficient, as a large number of neurons are encoding the same information.

3.4 Information theory

Figure 6 shows that for the three parameters we tested, biological neuronal networks tend to organize at the transition between asynchronous firing and distinct network bursting. From an information theoretic perspective, a synchronous network is highly redundant since each neuron is not encoding new information. However, such networks are robust with respect to noise in the network. Conse-

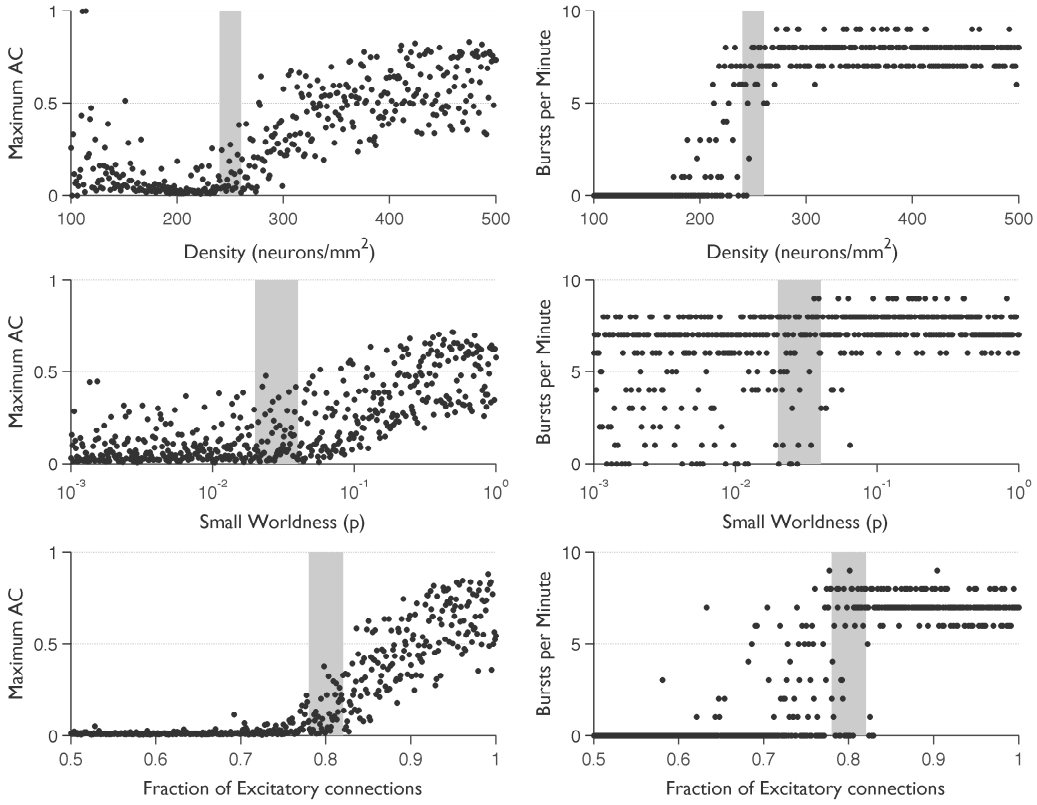

Figure 6: Analysis of bursting metrics across parameters. The maximum AC parameter (left) and the bursts per minute count (right) are shown for different values of density (top), small-world parameter (middle), and fraction of excitatory synapses (bottom). For all three parameters, both the maximum AC component of the GFR and the number of bursts per minute are found to increase along with the parameter, indicative of an emergence in the strength and synchrony of network bursting. Grey bars indicate typical values of the parameters from networks in culture.

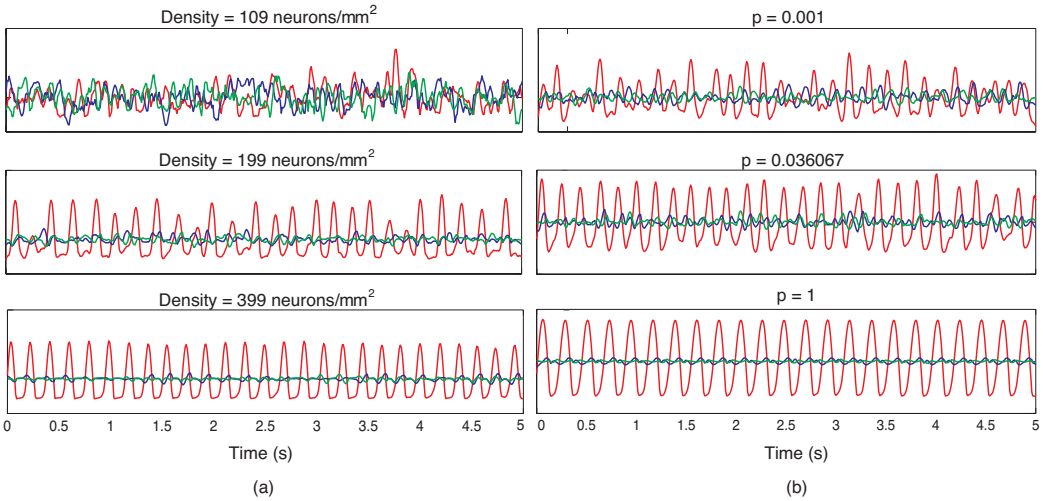

Figure 7: Neural trajectories across time. First (red), second (blue), and third (green) principal components of the firings rates are shown across time for different values of density (a) and p (b).

quently, we hypothesized that these critical regions allow the network to represent a large amount of information with enough redundancy such that the information capacity of the network is maximized even in the presence of noise. To test this, we estimated the information capacity of simulated networks of various densities, connection types, and inhibitory/excitatory ratios. Figure ??? shows the information of networks of differing parameters. The information capacity peaks around the typical parameter values seen in neural system, supporting the hypothesis that networks attempt to self-maximize the amount of information that they can accurately carry in the presence of random background noise.

4 Discussion

These results help to uncover the nature of network bursting observed in *in vitro* cultures. Bursting appears to be an emergent property of networks with both excitatory and inhibitory connections. Simulations qualitatively match data obtained from cultures grown on microelectrode arrays, and are able to mimic the wide repertoire of activity seen experimentally. The model was developed using a bottom-up approach, replicating both the connectivity and intrinsic properties observed in in vitro cultures. Random synaptic noise appears to be a sufficient

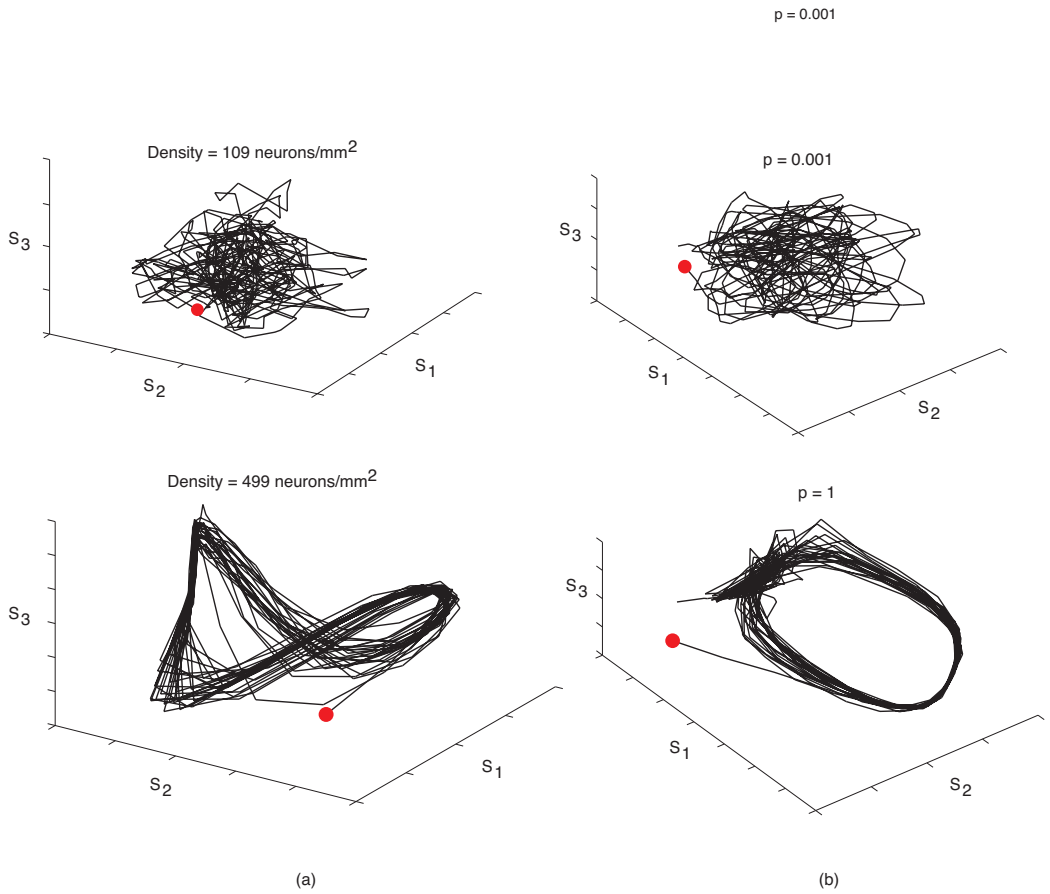

Figure 8: Trajectories through state space. Neural trajectories (black lines) projected onto the first three principal components shown for different densities (a) and values of p (b). Initial states are marked with a red dot.

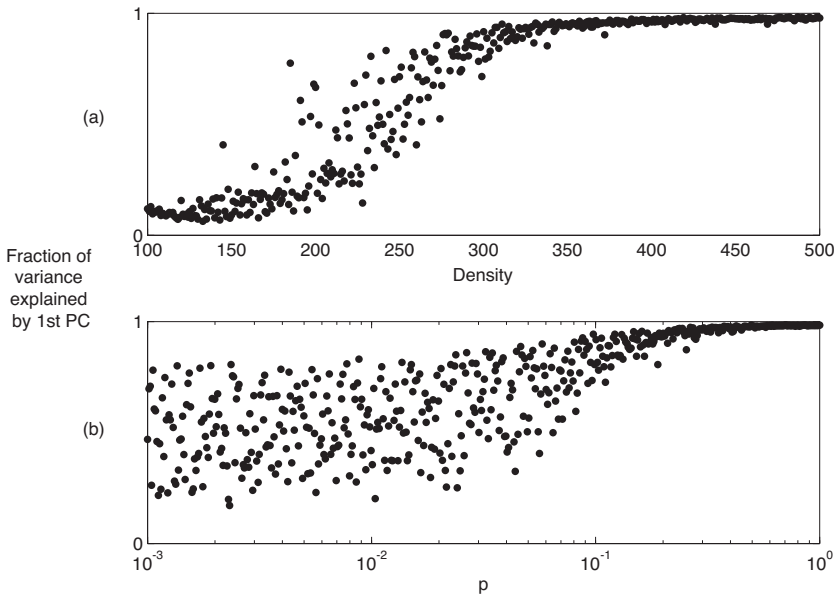

Figure 9: Fraction of the variance captured by the first principal component across different values of density (a) and small-world rewiring probability p (b).

input for driving these cultures towards self-synchronization.

4.1 Bursting

The dynamics of network bursting are explored across the parameter space, against both the density of the network and the type of connections (realized by the small world rewiring probability p). The strength and periodicity of bursting is found to become more prominent as the density increases or as the network becomes more random and disorganized. This gradation in strength of bursting has been observed experimentally by Wagenaar et al., and has qualitatively been shown to depend on plating density [12]. Ideally, the activity from these simulations will in turn make predictions regarding the dynamics of cultured neuronal networks. Certain network properties (neuronal dynamics, individual connections and weights, neuron locations and type) are randomized at the beginning of a simulation, indicating that these individual parameters do not affect global network behavior. Our findings show that network bursting is a connection-dependent, large-scale phenomenon and is independent of the differences in individual neurons and their connections.

Projecting network firing rates onto an optimal subspace using principal components analysis yields more insight into the dynamics of network bursting. As density is increased, or as the network connections becomes more long-range, the amount of variance captured by the first principal component increases markedly from as little as 10% to as much at 95%. This implies that networks with a strong degree of bursting are highly redundant such that the behavior of all of the neurons can be captured with only a few. Trajectories of the neural state through the phase space of the top three components show that the dynamics are chaotic and unpredictable for sparse or ordered cultures, yet for dense or random cultures, distinct limit cycle attractors arise. These attractors are robust with respect to random initialization of different networks, indicating that their dynamics are capturing the essential activity of the network. Persistent dynamical attractors have already been observed in experimental cultures [12]. Interestingly, the trajectories for dense networks are different from those of highly disorganized networks, which could serve as a potential marker for identifying experimental network states. The concept of thinking about network dynamics as a low dimensional projection of the higher order system proves to be very useful in understanding the behavior of the model.

4.2 Neural Code and Self-Organized Criticality

These observations from studying the principal components of the data allow us to speculate on issues of neural coding. From an information theory point of view, network bursting seems to be a redundant way of coding information when large numbers of neurons are used to represent information that could be carried with just one or two. This is supported by Figure xx. However, there is a tradeoff between capacity and robustness, as these dense networks are relatively unscathed with respect to noise or the removal of a subset of neurons. Thus, one might expect biological neural networks to remain in between these two extremes, taking advantage of robustness in the system while still utilizing the capacity efficiently. Interestingly, the simulations seem to support this idea; typical biological networks have densities of around 200-250 neurons/mm^2 and have characteristically small-world connections (corresponding to a p value of around 0.03). Note that for these values, the MAC parameter, bursts per minute count, and amount of variance captured through the first principal component all show a balance between too much order (strong bursting) and too much chaos (no bursting). These findings support the concept of self-organized criticality, originally proposed by Bak and colleagues [2] in which biological complexity arises from systems that

self-organize around critical transition points in the system's dynamics. Although speculative, the model results for typical parameter values reveals a network that teeters between chaotic asynchronous behavior and distinct bursts.

Why are these questions regarding network bursting important? Ideally, stuyding the dynamical properties of these simulated networks will give us insight into the dynamics of neuronal circuits in the brain. For example, although highly synchronous behavior is observed *in vitro*, it is only observed *in vivo* in pathalogical states, such as during epileptic seizures. Assuming these seizures consist of the network getting stuck at some attractor might lead to the discovery of new electrical stimulation techniques that could bump the network into a new basin of attraction. These ideas could develop into new forms of treatment for those who suffer from epilepsy. In addition, there are a number of engineering and control systems that look to utilize the high-dimensional dynamical processing that occurs in such networks, and understanding the mechanisms behind these neural systems could serve as the foundation for the development of new approaches for optimal control that more closely mimic those seen in biological systems.

5 Appendix

5.1 Description of Model

In developing the model, the general approach consisted of simulating a medium of spiking neurons, constraining the parameters of the model using what is known biologically about cortical cultures, and then comparing simulated activity to experimental data.

5.1.1 Neuron Model

The neuron model used is that proposed by Izhikevich [6], which is a type of quadratic integrate-and-fire neuron model. This model is both computationally efficient and can implement a wide repertoire of neuronal spiking dynamics [7]. The model consists of a fast acting variable describing the membrane voltage (v) and a slowly decaying membrane reset variable (u) defined by the following equations:

$$\frac{dv}{dt} = 0.04v^2 + 5v + 140 - u + I \quad (1)$$

$$\frac{du}{dt} = a(bv - u) \quad (2)$$

With the after-spike reset conditions:

$$\text{if } v \geq +30mV, \qquad then \begin{cases} v \leftarrow c \\ u \leftarrow u + d \end{cases}$$

The parameters a, b, c, and d are dimensionless variables that are chosen to give the neurons various spiking dynamics, and the current I is composed of a noise component and the synaptic current due to neurotransmitter release from presynaptic neurons. Varying the dimensionless parameters a through d allows for tuning of the spiking behavior of the neurons.

5.1.2 Synaptic Release

Neurons form connections at synapses which are modeled by a simple exponentially decaying neurotransmitter (n) release, defined by the following:

$$\frac{dn}{dt} = -\frac{n}{\tau_n} \tag{3}$$

This model is efficient in capturing the decay in neurotransmitter at the synapse after a spike. Axonal delays, which have been found to have a wide range of distinct values in cortical neurons, are also incorporated into the model as randomly chosen values drawn uniformly from the range of $1ms$ to $20ms$. Specific timings of presynaptic spikes are required to force a postsynaptic spike, otherwise they potentiate the postsynaptic neuron.

5.1.3 Small World Connections

Connections between neurons are chosen according to the small world paradigm [13]. Neurons are initially wired to every neuron within some radius threshold σ, and then randomly rewired to other neurons across the network with probability p. A value of $p = 0.03$ was chosen to obtain a short mean path length and high clustering coefficient. This process yields sparse synaptic weight distributions which are then initialized to randomly chosen weights, drawn from normal distributions. Typically, 80% of the synapses are chosen to be excitatory and 20% are chosen to be inhibitory. This ratio is pervasive through cortical tissue [REFERENCE].

5.1.4 Microelectrode Arrays

Although computer simulation monitors the activity of all the neurons in the network, MEA electrodes would only capture a subset of the activity. In order to

mimic extracellular recordings from the network, the electrode interface was also modeled. A given electrode records spikes from all neurons overlapping the electrode. The electrode activity can be thought of as a spatial subsampling of the activity of the underlying network.

5.2 Data metrics

In order to analyze the bursting behavior observed in the networks, two metrics are used. To compute them, the network spikes are summed into discrete time bins and then smoothed to obtain a time-varying signal representing the average firing rate of the network, called the global firing rate (GFR). The first metric consists of using a peak detection algorithm to determine the number of peaks in the GFR signal per minute, which is defined as the number of bursts per minute (BPM). The second metric is simply the value of the maximum AC component (MAC) of the fourier transform (computed via the FFT) of the GFR. The MAC is meant to be a measure of the amount of periodic bursting in the network - a large AC component in the FFT is indicative of a high degree of periodicity.

5.2.1 Principal Components Analysis

Previous work [4] has used dimensional reduction techniques to project firing rates onto low-dimensional variables that allow for easier visualization of neural trajectories. The general idea is that redundancy is encoded in the firing rates of neurons, so using a PCA-like method to transform the firing rates onto a basis that better captures the variance in the data allows us to ignore the redundant variables. To extract neural trajectories, the firing rates for individual neurons were first determined by binning spike counts into $10ms$ time windows. The square root of the rates was taken (to compress the range) and then smoothed by convolving the signals with a Gaussian kernel. PCA was run on these smoothed firing rate trajectories, and the top three components were extracted to serve as the low-dimensional projection of the neural state.

5.2.2 Information estimates

Information capacity was estimated using the method described by Yu et. al.[14]. It consists of treating each spike train as a series of M delta functions, where each is shifted to the location of a given spike and M is the total number of spikes in the spike train.

$$s(t) = \sum_{i=1}^{M} \delta(t - t_i) \tag{4}$$

The fourier transform of a set of such delta functions is a sum of sines and cosines whose frequency depend on the timing of the delta function.

$$F[s(t)](k) = \sum_{i=1}^{M} e^{-2\pi i k t_i} = \sin(2\pi k t_i) - i\cos(2\pi k t_i) \tag{5}$$

These fourier coefficients allow for estimation of the entropy at each frequency in the network. With enough data, the set of fourier coefficients at a given frequency approaches a normal distribution according to the central limit theorem. The entropy of a normal distribution is easily computed given the variance of that distribution.

$$H(\sigma^2) = \frac{1}{2}\log 2\pi e\sigma^2 \tag{6}$$

Thus, the variance of the fourier coefficients at a given frequency allow us to estimate the entropy of the network at a given frequency. The total entropy of the network is given by summing across all frequencies. This ends up giving a general estimate of the total entropy of a system, if the input is random noise. However, given a repeated stimulus, the computation described above yields just the noise entropy. To estimate the information of the network, a simulation was run with random noise and another was run with a repeated stimulus. The different in entropy between the two was used as the measure of the information of the network.

References

[1] S Achard, *A Resilient, Low-Frequency, Small-World Human Brain Functional Network with Highly Connected Association Cortical Hubs*, Journal of Neuroscience **26** (2006), no. 1, 63–72.

[2] P Bak, *Self-organized criticality*, Scientific American (1991).

[3] Chuanping Chen, Lin Chen, Yunsheng Lin, Shaoqun Zeng, and Qingming Luo, *The origin of spontaneous synchronized burst in cultured neuronal networks based on multi-electrode arrays.*, Bio Systems **85** (2006), no. 2, 137–143.

[4] Mark M Churchland, Byron M Yu, Maneesh Sahani, and Krishna V Shenoy, *Techniques for extracting single-trial activity patterns from large-scale neural recordings.*, Current Opinion in Neurobiology **17** (2007), no. 5, 609–618.

[5] Felipe Gerhard, Gordon Pipa, Bruss Lima, Sergio Neuenschwander, and Wulfram Gerstner, *Extraction of Network Topology From Multi-Electrode Recordings: Is there a Small-World Effect?*, Frontiers in Computational Neuroscience **5** (2011).

[6] E M Izhikevich, *Simple model of spiking neurons*, IEEE Transactions on Neural Networks **14** (2003), no. 6, 1569–1572.

[7] _____, *Which Model to Use for Cortical Spiking Neurons?*, IEEE Transactions on Neural Networks **15** (2004), no. 5, 1063–1070.

[8] Valentina Pasquale, Sergio Martinoia, and Michela Chiappalone, *A self-adapting approach for the detection of bursts and network bursts in neuronal cultures*, Journal of Computational Neuroscience **29** (2009), no. 1-2, 213–229.

[9] S M Potter and T B DeMarse, *A new approach to neural cell culture for long-term studies.*, Journal of Neuroscience Methods **110** (2001), no. 1-2, 17–24.

[10] Jonathan V Selinger, Nadezhda V Kulagina, Thomas J O'Shaughnessy, Wu Ma, and Joseph J Pancrazio, *Methods for characterizing interspike intervals and identifying bursts in neuronal activity*, Journal of Neuroscience Methods **162** (2007), no. 1-2, 64–71.

[11] O Sporns, *The small world of the cerebral cortex*, Neuroinformatics (2004).

[12] Daniel Wagenaar, Zoltan Nadasdy, and Steve Potter, *Persistent dynamic attractors in activity patterns of cultured neuronal networks*, Physical Review E **73** (2006), no. 5.

[13] D J Watts and S H Strogatz, *Collective dynamics of 'small-world' networks.*, Nature **393** (1998), no. 6684, 440–442.

[14] Yunguo Yu, Marshall Crumiller, Bruce Knight, and Ehud Kaplan, *Estimating the amount of information carried by a neuronal population.*, Frontiers in Computational Neuroscience **4** (2010), 10.